İSTANBUL UNIVERSITY PRESS

European Journal of Biology

Research Article

Open Access

The Effects of the Major Phytochemicals of *Salvia miltiorrhiza* on the Serine Protease KLK-5 in Rosacea: *In Silico* Screening and Molecular Dynamics Simulation

Sumeyye Durmaz[1] & Esma Ulusoy[2]

[1] Uskudar University, Institute of Science, Molecular Biology, Istanbul, Türkiye
[2] Uskudar University, Faculty of Engineering and Natural Sciences, Molecular Biology and Genetics, Uskudar, Istanbul, Türkiye

Abstract

Objective: Rosacea is a chronic inflammatory skin disorder in which kallikrein-5 (KLK-5) plays a crucial role in disease progression. Targeting KLK-5 inhibition is a promising therapeutic strategy. Regarding rosacea's complex mechanisms and pathophysiology, KLK-5 plays a key role in the immune dysregulation pathway. The pathophysiology of rosacea may begin with an aberrant innate immune response, marked by overexpressed and over-activated KLK-5, which increases the expression of Toll-like Receptor 2 and MMP-9. The cleavage of larger precursor peptides into LL-37 leads to inflammation.

Materials and Methods: This study investigated the major phytochemicals of *Salvia miltiorrhiza* as potential KLK-5 inhibitors through molecular docking, ADME-Tox analysis, and molecular dynamics (MD) simulations. Docking studies assessed the binding interactions of *S. miltiorrhiza* phytochemicals with KLK-5 (PDB ID: 6QFE), comparing them to a native ligand (GSK144) and the clinically used azelaic acid.

Results: Azelaic acid exhibited the weakest binding affinity, whereas danshensu, tanshinone I, and tanshinone IIA demonstrated stronger interactions with KLK-5. The ADME-Tox analysis identified danshensu as the most promising candidate owing to its favorable pharmacokinetic and toxicity profiles. MD simulations further confirmed the stability of the danshensu-KLK-5 complex, showing minimal structural fluctuations and supporting its inhibitory potential.

Conclusion: These findings indicate that danshensu is a promising candidate for KLK-5 inhibition in rosacea, suggesting the need for further studies to validate its therapeutic potential.

Keywords Rosacea · *Salvia miltiorrhiza* · Molecular Docking · ADME-Tox · Molecular Dynamics Simulation · Computer-Aided Drug Design

Corresponding author: Esma Ulusoy esma.ulusoy@uskudar.edu.tr

INTRODUCTION

Rosacea is a common chronic skin inflammatory condition affecting over 45 million individuals globally, primarily affecting the middle part of patients' faces.[1-3] Its defining features are erythema, papules, pustules, telangiectasia, or a combination of these symptoms. The four clinical subtypes of rosacea—ocular, phymatous, papulopustular, and erythematotelangiectatic—are identified by the National Committee of Experts.[4] The clinical manifestations of rosacea are varied according to the patient's symptoms. It is characterized by redness, peeling, itching, and pustules.[5-7] Although the exact cause of rosacea is unknown, several factors are known to play a role in its development. In the innate immune system, neurovascular dysfunction and anomalies are two primary factors that trigger the development of rosacea.[3,4,7] In this manner, innate immunity involves the skin's physical barrier, antimicrobial peptides, and pattern recognition receptors.[4,7-9] Patients with rosacea have an altered innate immune system. At this point, it is known that the skin is vital to balancing innate immunity by functioning as a host defense mechanism, and since innate immune system disorders raise skin sensitivity against environmental stimuli, it is hypothesized that it may play a role in the development and severity of rosacea (Figure 1).[4,7,10]

Furthermore, according to recent genetic research, a variety of genetic variations, including those related to inflammation, vascular biology, and immunological control, are connected to rosacea.[4,7,10-12] Therefore, in the development of rosacea, hereditary factors may play a role. Other significant factors that trigger rosacea include heat, stress, Demodex colonization, and ultraviolet light. The effects of ultraviolet light, heat, Demodex mites, and stress can lead to the release of pro-inflammatory mediators, which can cause the onset or worsening of rosacea symptoms (Figure 1).[4,7,10-12] Many researchers recognize neurovascular dysfunction, a weakened skin barrier, and immune system imbalance as key contributors to the intricate pathophysiology of rosacea, resulting in both eye and skin symptoms.[3,4,7] Nonetheless, the exact mechanisms that cause the onset of rosacea remain unclear. The complicated mechanism of rosacea involves endogenous factors such as genetic predispositions and cellular stress responses[4,7,13], as well as exogenous factors like histamine-rich foods, alcohol, and spicy foods.[3,4,7,14] It also encompasses immune system dysregulation[4,7,14], including adaptive immune responses[4,7,15], neuroimmune, vascular, and neurovascular dysregulation[7,16,17], along with the innate immune system[4,7,18,19].

The defining characteristics of rosacea include innate and adaptive immune dysregulation. Among the various underlying mechanisms of rosacea, the most extensively researched involves the pathways of Toll-like Receptor 2 (TLR2)/serine protease kallikrein-5 (KLK-5)/LL-37.[4,7,18,19] As members of the transmembrane receptor family, Toll-like receptors located in keratinocytes and fibroblast cells play a crucial role in recognizing both chemical and physical stimuli and microbial infections. Additionally, these receptors are present in cells of the innate immune system, including mast cells and phagocytes.[18,19] TLR activation by stimuli triggers the innate immune system, producing cathelicidins, chemokines, and cytokines by regulating nuclear factor-κB signaling.[4,7,20,21] As a result, excessive TLR activation can lead to abnormal inflammation.[4,22] The activation of the innate immune system through the overactivation and overexpression of TLR-2 leads to an increased production of cathelicidins.[4,20] These peptides are vital components of antimicrobial peptides that help
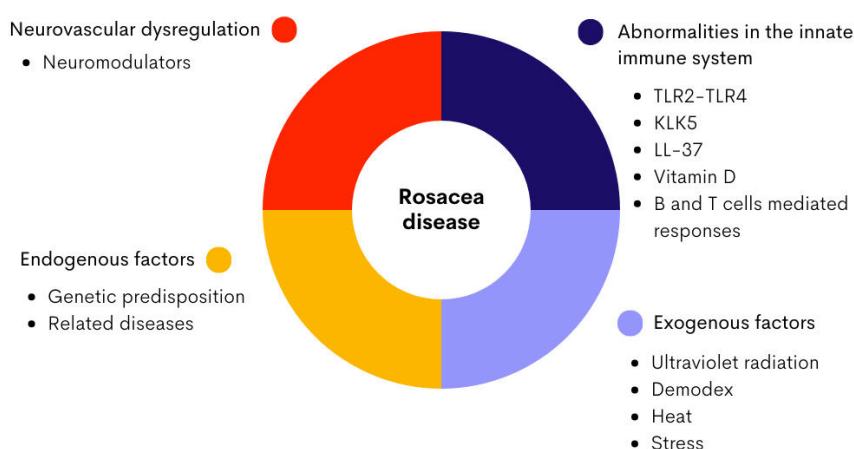

Figure 1. Scheme of the major contributory factors for rosacea disease.

regulate innate immunity in mammals.[23,24] In this context, LL-37 is one of the most significant antimicrobial peptides leading to inflammation via the TLR-2/KLK-5 pathway. Studies on rosacea skin biopsies have shown increased LL-37 expression. At the same time, KLK-5 is also significantly expressed in the skin of patients with rosacea, similar to its role in other dermatological disorders like Netherton syndrome and atopic dermatitis.[4,6,23–25] Therefore, it is evident that LL-37 is excessively produced in the skin of patients with rosacea because of the increased expression of KLK-5.[26–29] Clinical signs of rosacea show increased expression of LL-37 and other peptides. Therefore, it is believed that treatments targeting KLK-5 function or reducing its production could inhibit the formation of LL-37 and irregular peptide fragments, potentially halting the clinical manifestations of rosacea.[4,28–30]

Rosacea treatment involves a combination of anti-inflammatory, antimicrobial, vascular-targeted, and psychological strategies.[6,7] Azelaic acid[7,31], hydroxychloroquine[7,31], and tetracycline[7,31,32] antibiotics effectively reduce inflammation. Meanwhile, IL-17 inhibitors and isotretinoin focus on modulating immune responses.[7,33] Antimicrobial options like rifaximin[7,34,35], omiganan[7,36], metronidazole[7,37,38], and ivermectin[7,39–41] are used against bacterial and *demodex*-related rosacea. Vascular-targeted therapies, such as timolol[7,42,43], brimonidine[7,44], and oxymetazoline [7,39–41] help manage erythema by constricting blood vessels and inhibiting angiogenesis. Additionally, psychological treatments that include paroxetine[7,45,46], and β-adrenergic blockers[7,47] (carvedilol[7,47,48] and propranolol [7,47,48]) address flushing and inflammation. Collectively, these strategies improve rosacea symptoms by targeting its diverse causes. In the context of major contributors, according to recent studies, rosacea is a dermatological disease that is controlled and worsened by overactivation of KLK-5. The cleavage of the 18-kDa cationic antimicrobial protein called the CAP-18 precursor into the antimicrobial peptide LL-37 promotes inflammation in the skin and eyes.[4,7] Recently, it has been stated that there are no specific inhibitors for KLK-5 available, except for azelaic acid, which is applied topically at a 15% concentration and has been observed to have action on KLK-5.[7,12] Thus, the identification and discovery of inhibitors of KLK-5 represent a potential way to treat rosacea.

Within the Lamiaceae family, one of the largest genera is *Salvia*.[49,50] Three distinct regions exhibit a diverse assortment of *Salvia* species: Central and South America display a total of 500 species, while Eastern Asia is home to 90 species, and Central Asia and the Mediterranean collectively encompass 250 species.[50] According to reports, it is expressed that *Salvia miltiorrhiza* is a species of *Salvia* genus found on the

hillside and understory grass locations at an altitude of 120–1300 meters in Shanxi, Anhui, Jiangxi, Sichuan, Zhejiang, and Hebei.[50] *S. miltiorrhiza*, commonly referred to as Danshen in China, has been used for millennia to treat cardiovascular disorders and neurasthenic insomnia in traditional Chinese medicine. It is also used to determine the medicinal components of Danshen Dripping Pill, the very first Chinese herbal medicine to receive Food and Drug Administration (FDA) approval for clinical trials in the United States.

The main phytochemical components of *S. miltiorrhiza,* triterpenoids, flavonoids, phenolic acids, diterpenoids, and saccharides are known.[49,50] According to a variety of high-performance liquid chromatography fingerprint and gas chromatography–mass spectrometry analyses conducted for *S. miltiorrhiza* by different research groups, tanshinone IIA, salvianolic acid B, cryptotanshinone, lithospermic acid, rosmarinic acid, danshensu, dihydrotanshinone, salvianolic acid A, and tanshinone I are found to be major phytochemical constituents of *S. miltiorrhiza*.[51–54] Therefore, it has been hypothesized that the discovery of this plant's active chemicals may eventually produce novel medications derived from these active components. *S. miltiorrhiza* is referenced in historical texts and is acknowledged as a medicinal species within academic research. The advantages of this method include its small genome size, ease of establishing *in vitro* tissue cultures, and straightforward cultivation methods. Researchers have examined its biosynthetic pathways and investigated its pharmacological effects, encompassing anti-fatigue, antidiabetic, and anti-Alzheimer properties across diverse models *in vitro* and *in vivo*.[50,55–57]

KLK-5, a serine protease, is vital in skin conditions, especially in rosacea development. Currently, there are not enough drugs designed to target KLK-5 specifically. The only known specific inhibitor of KLK-5 in the literature is azelaic acid, which is effective at 15% concentration when used topically. Hence, the identification of KLK-5 inhibitors is crucial for the development of new treatment alternatives. In the present study, we propose, for the first time, that major components of *S. miltiorrhiza* inhibit KLK-5 activity, that these compounds are promising candidates for KLK-5-targeting therapies.

MATERIALS AND METHODS

Molecular Docking Preparation

The target selection for this study was the role of KLK-5 in the development of rosacea. We screened the Protein Data Bank (PDB) and selected human KLK-5 using the PDB ID: 6QFE. For our molecular docking studies, we identified the KLK-5 active site based on previous research. After obtaining the 3D crystallized structure of KLK-5 from the Protein

Data Bank, we prepared and energy-minimized the protein using BIOVIA Discovery Studio 2016 software (https://www.3ds.com/products-services/biovia/). *S. miltiorrhiza*'s primary components and native KLK-5 ligand (PubChem CID: 138115400) have been recognized as ligands for molecular docking research. We obtained their 2D or 3D structures from the PubChem database (https://pubchem.ncbi.nlm.nih.gov/). These structures were provided in ".sdf" format and converted into 3D ".pdb" format using PyMOL 2.5 (https://pymol.org/2/). The ligands were then prepared for molecular docking using AutoDock Tools 1.5.7 (MGL Tools 1.5.7) (https://ccsb.scripps.edu/mgltools/). Additionally, we used azelaic acid (DrugBank ID: DB00548) as a reference ligand, which was obtained from the DrugBank database (https://go.drugbank.com/). The same preparation process was used for the azelaic acid compound. We conducted molecular docking to explore the interactions between the phytochemical constituents of *S. miltiorrhiza* and the receptor KLK-5 (PDB ID: 6QFE). "Structure-Based Virtual Screening" studies were performed using AutoDock Vina 1.1.2 software (https://vina.scripps.edu/), with specific coordinates defined for the active region at (x: –3.48, y: –15.17, z: 67.76).[30] The Grid Box size was set to (40x40x40 Å) based on the active region of 6QFE. We selected the best-generated poses based on the docking scores after docking the chosen ligands against the receptor proteins.

ADME-Tox (Absorption, Distribution, Metabolism, Excretion, Toxicity) Analysis

In addition to docking studies, we analyzed ADME-Tox (absorption, distribution, metabolism, excretion, toxicity) scores to evaluate the compatibility of the candidate ligands. This analysis is crucial to the drug discovery and development processes. We used the web-based tools SwissADME (http://www.swissadme.ch/) and ProTox-II (http://tox.charite.de/protox_II) for this assessment.

Molecular Dynamics (MD) Simulation

The MD simulation method was employed to simulate the top five ranked ligand-protein complexes, running for 150 ns at a temperature of 309.15 K (36°C). A timestep of 2 femtoseconds was used for the simulation. Additionally, the apo structure of KLK-5 was simulated using the same parameters. Prior to the molecular dynamics simulations, the CHARMM36m Force Field generated the CHARMM topology and parameter files. Using CHARMM-GUI, the topology and parameter files for both the ligand and the protein were established. Ions, specifically KCl, were added to the simulation box to achieve the desired ion concentration, and the system was neutralized by incorporating K^+ and Cl^- ions. The simulation preparations

were conducted at a temperature of 309.15 K (36°C). Once the input parameters and files were prepared, the molecular dynamics simulation was executed using NAMD (NAMD 2.4) via the TRUBA e-infrastructure. Furthermore, analyses such as root mean square fluctuation (RMSF), radius of gyration (Rg), and root mean square deviation (RMSD) were performed to evaluate the stability of the receptor-ligand system.

RESULTS

The results of protein-ligand molecular docking for 11 ligands are presented alongside the predicted ADME-Tox properties of the selected ligands based on established docking score thresholds. In addition, 3D structures that illustrate the protein-ligand interactions of these selected ligands are included. In addition to the molecular docking and ADME-Tox assessments, we also present the MD simulation results. Analyses of RMSD, RMSF, and Rg were conducted to identify promising compounds for further *in vitro* and *in vivo* studies.

Molecular Docking Results

To identify the hit compounds, molecular docking studies were conducted using AutoDock Vina. Table 1 summarizes the estimated binding free energy (kcal/mol) of the identified ligands obtained from the PubChem and DrugBank databases. This table also displays the 2D chemical structures of the ligands along with their PubChem IDs. Table 1 presents the affinity scores obtained from molecular docking studies of ligands as potential inhibitors for the target protein 6QFE. These scores reflect the interaction strength between each ligand and the target protein, providing insights into the ligand's ability to bind effectively. To validate the molecular docking results, we conducted docking experiments using the native ligand GSK144 with the target protein. According to Table 1, salvianolic acid B exhibits the highest affinity for the target, whereas azelaic acid, which inhibits KLK-5, had the lowest affinity.

SwissADME Analysis Results

The ligand library's drug similarity, pharmacokinetic, physicochemical, and medicinal chemistry properties were analyzed using the SwissADME tool. Results, including chemical structure, size, solubility, lipophilicity, polarity, saturation, and flexibility, are summarized in Table 2 and represented in the Bioavailability Radar (Figure 2). Additionally, the BOILED-Egg model (Figure 3) shows forecasts for GIA and blood-brain barrier (BBB) permeation of ligands. According to Figure 3, Molecule 1 (salvianolic acid B) and Molecule 2 (lithospermic acid) fall outside the defined range and are not included in the BOILED-Egg model.

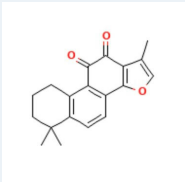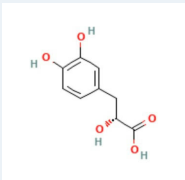**Table 1.** The molecular docking outcomes of 6QFE with eleven identified ligands.
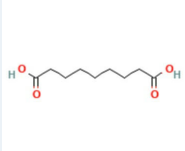
Ligand Names	PubChem Compound ID	2D Chemical Structure	Estimated Free Energy of Binding ΔG (kcal/mol)
Salvianolic acid B	6451084		−9.9
GSK144	138115400		−9.6
Lithospermic acid	6441498		−9.3
Salvianolic acid A	5281793		−9.3
Rosmarinic acid	5281792		−8.4
Cryptotanshinone	160254		−8.0
Tanshinone IIA	164676		−7.9
Tanshinone I	114917		−7.8
Dihydrotanshinone	5316743		−7.6

Table 1. Continued.

Ligand Names	PubChem Compound ID	2D Chemical Structure	Estimated Free Energy of Binding ΔG (kcal/mol)
Danshensu	11600642		−7.2
Azelaic acid	2266		−4.0

Both are predicted not to penetrate the BBB or to be absorbed, as indicated by total polar surface area values of 278.04 and 211.28 Å², respectively (Table 2). Molecule 3 (salvianolic acid A) and Molecule 4 (rosmarinic acid) are also outside the acceptable range, suggesting they are not BBB penetrant and will not be absorbed through the gastrointestinal tract because they do not fall within the egg model (Figure 3 and Table 2). In contrast, molecules 5 (cryptotanshinone) and 6 (tanshinone IIA) are predicted to be BBB penetrants. However, they are substrates of P-glycoprotein (P-gp), meaning they are actively effluxed from the brain, as indicated by blue dots in the yellow region of the plot. Molecules 7 (tanshinone I) and 8 (dihydrotanshinone) are anticipated to penetrate the brain because they are not substrates for P-glycoprotein, indicating that they are not actively expelled. Molecule 10 (azelaic acid) is expected to cross the BBB passively, as evidenced by its location in the yellow area and the presence of a red dot, which suggests that it is not expelled from the brain. On the other hand, Molecule 9 (danshensu), situated in the white region and indicated with a red dot, is predicted not to reach the brain. It is expected that it will be effectively absorbed through the gastrointestinal tract but will not be actively effluxed. Table 2 outlines Lipinski's Rule of Five (RO5) violations: salvianolic acid B and lithospermic acid each have three violations, whereas Salvianolic acid A has one. The remaining ligands did not exhibit any violations. Predictions for the water solubility of the ligands are based on the ESOL prediction model, and skin permeability is indicated by the permeability coefficient (Kp). Additionally, the human intestinal absorption and BBB permeability estimations for the ligands are presented in Figure 2 and Figure 3.

ProTox-II Analysis Results

An *in silico* study using the ProTox-II web server was conducted to examine the toxicity profiles of 10 ligands. This analysis covered toxicological pathways, toxicity classes, organ toxicity, and toxicity endpoints using computational estimations. The predictions of these ligands are presented in Table 3 and illustrated in toxicity radar graphics (Figure 4).

In the oral toxicity classification model, Classes I and II represent the highest levels of hazard and toxicity, whereas Class VI is recognized as the least harmful category, which is determined by the predicted lethal dose that results in the death of half of the tested animals. According to Table 3, salvianolic acid B and lithospermic acid are projected to fall into Class II, indicating that they may be fatal if ingested. Tanshinone IIA, tanshinone I, danshensu, and azelaic acid are predicted to belong to Class IV, they could be harmful when swallowed. Additionally, salvianolic acid A and rosmarinic acid are anticipated to fall into Class V, which may pose hazards if ingested. In comparison, cryptotanshinone and dihydrotanshinone are classified as Class VI, suggesting they are likely non-toxic. Additionally, the organ toxicity parameters indicated that all nine ligands are likely non-hepatotoxic, similar to azelaic acid, known for its effectiveness against KLK-5 in the treatment of rosacea. According to toxicity reports, all ligands were assessed as non-cytotoxic, except for salvianolic acid B and lithospermic acid. The remaining ligands, alongside azelaic acid, are predicted to be non-mutagenic. However, cryptotanshinone and dihydrotanshinone are estimated to carry a carcinogenic risk. Importantly, besides danshensu, tanshinone IIA, azelaic acid, and tanshinone I, all other ligands are predicted to have immunotoxic effects.

Table 2. The representation of the pharmacokinetics of ligands.

Pharmacokinetic Parameters / Ligands	MW (g/mol) (≤500)	MLogP (≤4.15)	HBA (≤10)	HBD (≤5)	Violation (Lipinski)	TPSA (Å²)	Water Solubility LogS (ESOL)	Log K_p (cm/s)	GIA	BBB Permeant
Salvianolic acid B	718.61	0.25	16	9	3	278.04	Poorly Soluble	−7.86	Low	No
Lithospermic acid	538.46	0.45	12	7	3	211.28	Moderately Soluble	−7.61	Low	No
Salvianolic acid A	494.45	1.34	10	7	1	184.98	Moderately Soluble	−6.53	Low	No
Rosmarinic acid	360.31	0.90	8	5	0	144.52	Soluble	−6.82	Low	No
Cryptotanshinone	296.36	2.36	3	0	0	43.37	Moderately Soluble	−5.41	High	Yes
Tanshinone IIA	294.34	2.24	3	0	0	47.28	Moderately Soluble	−5.02	High	Yes
Tanshinone I	276.29	1.82	3	0	0	47.28	Moderately Soluble	−5.37	High	Yes
Dihydrotanshinone	278.30	1.93	3	0	0	43.37	Soluble	−5.75	High	Yes
Danshensu	198.17	−0.04	5	4	0	97.99	Very Soluble	−7.65	High	No
Azelaic acid	188.22	1.25	4	2	0	74.60	Very Soluble	−6.33	High	Yes

Abbreviations: MW: Molecular Weight, MlogP: Lipophilicity, HBA: Hydrogen Bond Acceptor, HBD: Hydrogen Bond Donor, TPSA: Topological Polar Surface Area, LogS: Solubility, $LogK_p$: Skin Permeation, GIA: Gastrointestinal absorption BBB: Blood-brain Barrier Permeability.

Analysis of Ligand-Protein Interactions

Based on an analysis of molecular docking, toxicity, and ADME results, the molecular interactions between danshensu, GSK144, tanshinone I, tanshinone IIA, and azelaic acid, as well as the target protein, were visualized. Selection of these ligands for the visualization of molecular interactions and subsequent molecular dynamics simulations based on drug-likeness and toxicity. The interactions between the native ligand and target protein were taken as a reference.

Based on the two-dimensional and three-dimensional interaction poses, as illustrated in Figure 5 and Figure 6, and based on the molecular interactions, the native ligand exhibits hydrogen bond interactions with SER190, SER195, SER214, ASP217, GLY216, and CYS220 within the binding site of KLK-5. Furthermore, GSK144 exhibited 13 hydrophobic interactions, which are highlighted in colors other than green. In consideration of the molecular interactions of the native ligand, a comparison was performed with the remaining ligand interactions present within the binding site of KLK-5. As depicted in Figure 5 and Figure 6, azelaic acid exhibited hydrogen bond interactions with HIS57 and SER195 and eleven hydrophobic interactions. Furthermore, tanshinone IIA reveals 5 hydrophobic interactions and one hydrogen bond interaction with TYR41. Similar to azelaic acid, tanshinone I exhibits the same H bonding interactions with HIS57 and SER195, while displaying 9 hydrophobic interactions. Lastly, danshensu exhibits twelve hydrophobic interactions, forming hydrogen bond interactions with HIS57, SER190, SER195, SER214, SER217, and GLY226 (Figure 5 and Figure 6). Certainly, when compared with the molecular interactions that the native ligand GSK144 forms within the binding pocket of KLK-5, it becomes apparent that danshensu establishes the same 5 hydrogen bond interactions that overlap with those formed by GSK144.

Results of Molecular Dynamics Simulations: Analysis of RMSD, RMSF, and Rg

To validate the results obtained from molecular docking, it is imperative to characterize and evaluate the stability of the molecular interactions formed during the docking process, in addition to confirming the conformational stability of the ligand-target protein binding, molecular dynamics simulations of five ligand-protein complexes (danshensu, GSK144, tanshinone IIA, azelaic acid, and tanshinone I) and the Apo structure of KLK-5 (PDB ID: 6QFE) were conducted for a duration of 150 nanoseconds (with a timestep of 2 femtoseconds) utilizing the NAMD software. RMSD, RMSF, and Rg analyses were performed for the Apo structure of KLK-5 and each ligand-protein complex.

As indicated in Figure 7, the average RMSD value for the Apo structure was measured at 1.14 Å. Furthermore, the average RMSD for the native ligand GSK144-protein complex was quantified at 2.47 Å. Among those ligand-protein complexes analysis, the danshensu-KLK-5 complex exhibited the highest stability, with an average RMSD value of 2.48 Å, which closely approximates the average RMSD values of both the native ligand-KLK-5 complex and Apo structure. When the Apo structure and all ligand-KLK-5 complexes are examined, it is observed that the complex with the highest average RMSD value of 4.0 Å, and consequently the least stable, was azelaic acid-KLK-5. Finally, the average RMSD values of tanshinone IIA-KLK-5 and tanshinone I-KLK-5 complexes are 2.9 Å and 3.3 Å, respectively.
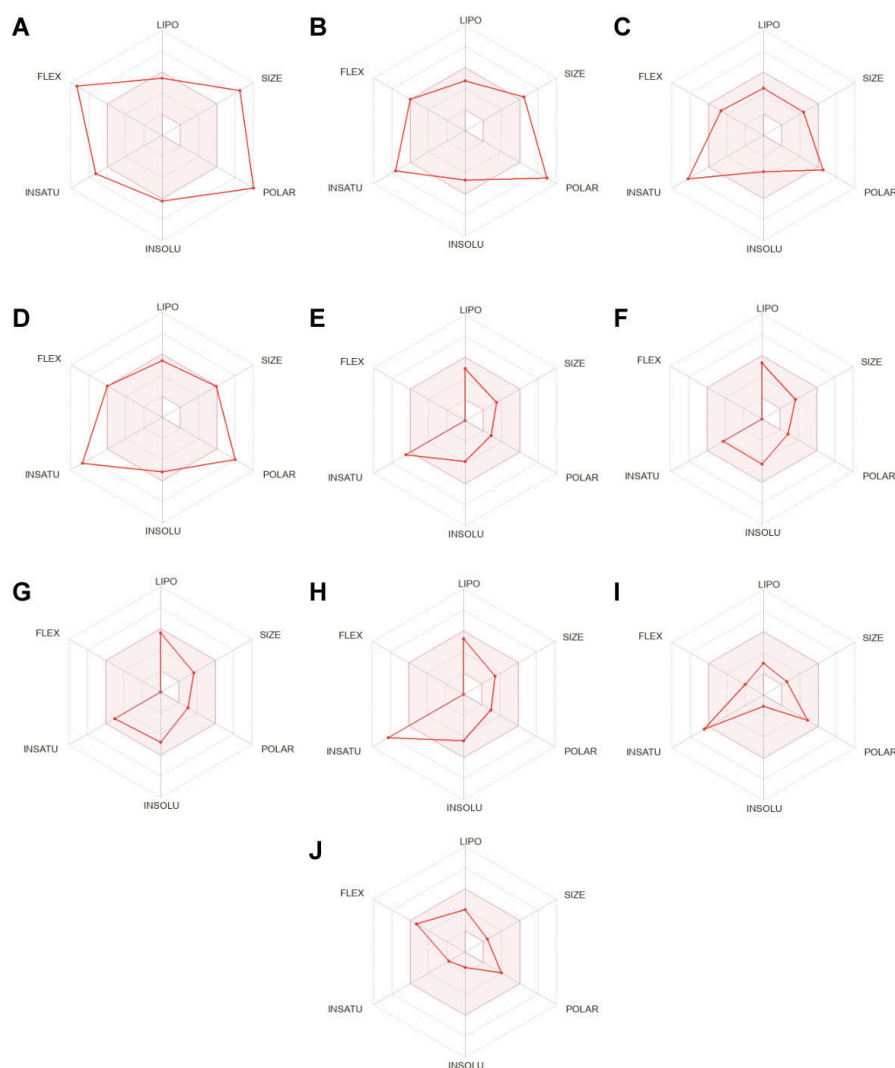
Figure 2. Bioavailability radar representations of ligands. (A) Salvianolic acid B, (B) Lithospermic acid, (C) Salvianolic acid A, (D) Rosmarinic acid, (E) Cryptotanshinone, (F) Tanshinone IIA, (G) Tanshinone I, (H) Dihydrotanshinone, (I) Danshensu, (J) Azelaic acid.
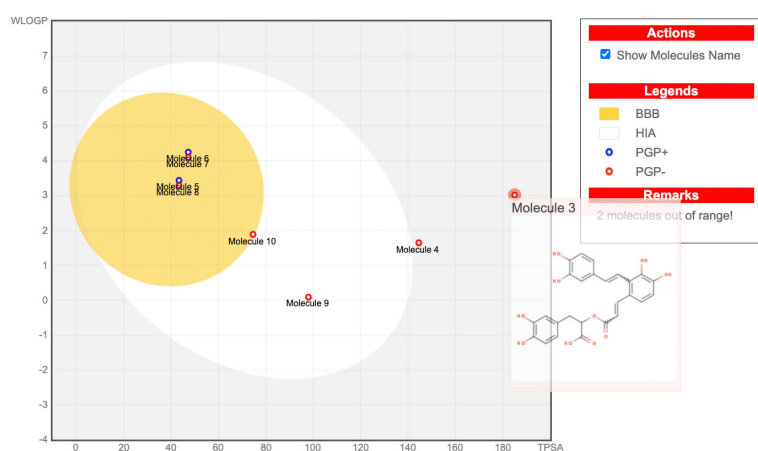

Figure 3. BOILED-Egg model predicts the GIA and BBB permeability of ligands. Molecule 1 (salvianolic acid B) and Molecule 2 (lithospermic acid) are excluded from the model as they fall outside the specified range. Molecules: 1: Salvianolic acid B, 2: Lithospermic acid, 3: Salvianolic acid A, 4: Rosmarinic acid, 5: Cryptotanshinone, 6: Tanshinone IIA, 7: Tanshinone I, 8: Dihydrotanshinone, 9: Danshensu, 10: Azelaic acid.

Table 3. The analysis of computational toxicity prediction of the 10 ligands was conducted using the ProTox-II web server. Ligands: 1: Salvianolic acid B, 2: Lithospermic acid, 3: Salvianolic acid A, 4: Rosmarinic acid, 5: Cryptotanshinone, 6: Tanshinone IIA, 7: Tanshinone I, 8: Dihydrotanshinone, 9: Danshensu, 10: Azelaic acid.

| Ligands Parameters	1	2	3	4	5	6	7	8	9	10
Toxicity Class	2	2	5	5	6	4	4	6	4	4
Predicted LD50 mg/kg	25	25	5000	5000	8000	1230	1655	8000	2000	900
Organ Toxicity										
Hepatotoxicity	Inactive	Inactive	Inactive	Inactive	Inactive	Inactive	Inactive	Inactive	Inactive	Inactive
Toxicity end points										
Carcinogenicity	Inactive	Inactive	Inactive	Inactive	Active	Inactive	Inactive	Active	Inactive	Inactive
Immunotoxicity	Active	Active	Active	Active	Active	Inactive	Inactive	Active	Inactive	Inactive
Mutagenicity	Active	Active	Inactive	Inactive	Inactive	Inactive	Inactive	Inactive	Inactive	Inactive
Cytotoxicity	Inactive	Inactive	Inactive	Inactive	Inactive	Inactive	Inactive	Inactive	Inactive	Inactive
Tox21-Nuclear Receptor Signaling Pathway										
Aryl hydrocarbon Receptor (AhR)	Inactive	Inactive	Inactive	Inactive	Inactive	Inactive	Active	Inactive	Inactive	Inactive
Androgen Receptor (AR)	Inactive	Inactive	Inactive	Inactive	Inactive	Inactive	Inactive	Inactive	Inactive	Inactive
Androgen Receptor Ligand Binding Domain (AR-LBD)	Inactive	Inactive	Inactive	Inactive	Inactive	Inactive	Inactive	Inactive	Inactive	Inactive
Aromatase	Inactive	Inactive	Inactive	Inactive	Inactive	Inactive	Inactive	Inactive	Inactive	Inactive
Estrogen Receptor Alpha (ER)	Inactive	Inactive	Inactive	Inactive	Inactive	Inactive	Inactive	Inactive	Inactive	Inactive
Estrogen Receptor Ligand Binding Domain (ER-LBD)	Inactive	Inactive	Inactive	Inactive	Inactive	Inactive	Inactive	Inactive	Inactive	Inactive
Peroxisome Proliferator-Activated Receptor Gamma (PPAR-Gamma)	Inactive	Inactive	Inactive	Inactive	Inactive	Inactive	Inactive	Inactive	Inactive	Inactive
Tox21-Stress response pathways										
Nuclear factor (erythroid-derived 2)-like 2/antioxidant responsive element (nrf2/ARE)	Inactive	Inactive	Inactive	Inactive	Inactive	Inactive	Inactive	Inactive	Inactive	Inactive
Heat shock factor response element (HSE)	Inactive	Inactive	Inactive	Inactive	Inactive	Inactive	Inactive	Inactive	Inactive	Inactive
Mitochondrial Membrane Potential (MMP)	Inactive	Inactive	Inactive	Inactive	Inactive	Inactive	Inactive	Inactive	Inactive	Inactive
Phosphoprotein (Tumor Suppressor) p53	Inactive	Inactive	Inactive	Inactive	Inactive	Inactive	Inactive	Inactive	Inactive	Inactive
ATPase family AAA domain-containing protein 5 (ATAD5)	Inactive	Inactive	Inactive	Inactive	Inactive	Inactive	Inactive	Inactive	Inactive	Inactive
Metabolism										
Cytochrome CYP1A2	Inactive	Inactive	Inactive	Inactive	Inactive	Inactive	Active	Active	Inactive	Inactive
Cytochrome CYP2C19	Inactive	Inactive	Inactive	Inactive	Inactive	Inactive	Inactive	Active	Inactive	Inactive
Cytochrome CYP2C9	Active	Active	Active	Active	Active	Active	Active	Active	Inactive	Inactive
Cytochrome CYP2D6	Inactive	Inactive	Inactive	Inactive	Inactive	Inactive	Inactive	Active	Inactive	Inactive
Cytochrome CYP3A4	Inactive	Inactive	Inactive	Inactive	Inactive	Inactive	Inactive	Inactive	Inactive	Inactive
Cytochrome CYP2E1	Inactive	Inactive	Inactive	Inactive	Inactive	Inactive	Inactive	Inactive	Inactive	Inactive
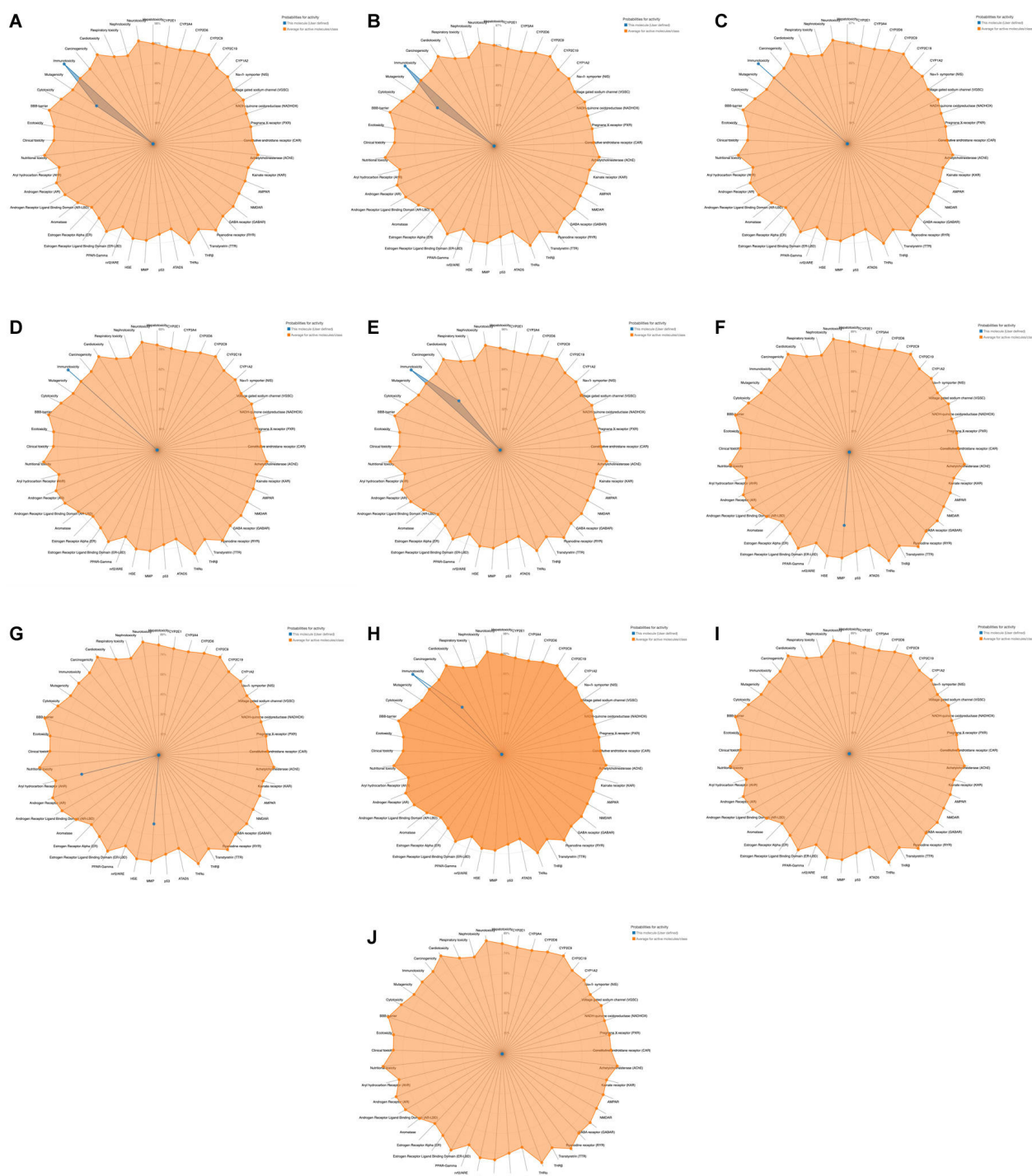
Figure 4. Toxicity radar graphics are represented as outputs of ProTox-II: (A) Salvianolic acid B, (B) Lithospermic acid, (C) Salvianolic acid A, (D) Rosmarinic acid, (E) Cryptotanshinone, (F) Tanshinone IIA, (G) Tanshinone I, (H) Dihydrotanshinone, (I) Danshensu, and (J) Azelaic acid.

RMSF analysis evaluates the local flexibility of the target protein, that regions with high RMSF values are more flexible. As illustrated in Figure 7, the ligand-target protein complexes exhibit comparable amino acid fluctuations in relation to the Apo structure. In each of the complexes, as well as in the Apo structure, high peaks are observed at similar residues: SER78, PRO37, ASN223, GLY79, GLU77, SER246, ASP185, ALA186, and PRO97, which are associated with the loop regions of KLK-5. In addition to these high peaks, the tanshinone IIA-KLK-5 complex exhibited a higher peak at MET24 than the other ligand-KLK-5 complexes. Furthermore, higher fluctuations are noted at the terminal end of the KLK-5 structure, which corresponds with the residue at SER246 and the adjacent
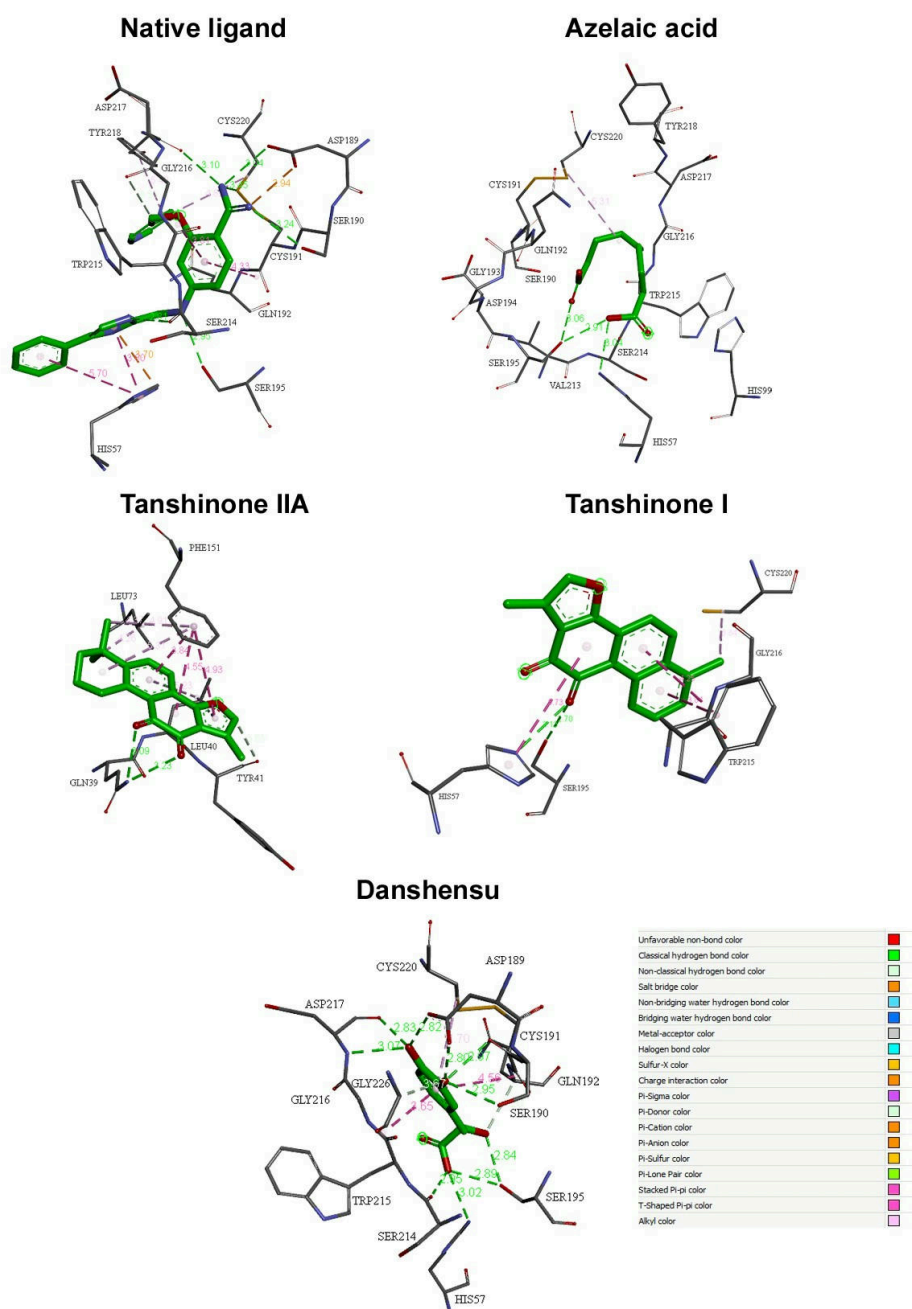
Native ligand

Azelaic acid

Tanshinone IIA

Tanshinone I

Danshensu

Unfavorable non-bond color	■
Classical hydrogen bond color	■
Non-classical hydrogen bond color	■
Salt bridge color	■
Non-bridging water hydrogen bond color	■
Bridging water hydrogen bond color	■
Metal-acceptor color	■
Halogen bond color	■
Sulfur-X color	■
Charge interaction color	■
Pi-Sigma color	■
Pi-Donor color	■
Pi-Cation color	■
Pi-Anion color	■
Pi-Sulfur color	■
Pi-Lone Pair color	■
Stacked Pi-pi color	■
T-Shaped Pi-pi color	■
Alkyl color	■

Figure 5. Detailed 3D interaction poses of the native ligand, azelaic acid, tanshinone IIA, tanshinone I, and danshensu within the KLK-5 binding site.

small loop structure; consequently, it aligns with the carboxyl end groups of the residue at SER246.

Rg measurements of five ligand-KLK-5 complexes, as well as the Apo structure, were presented to evaluate the stability of the ligand-target complexes (Figure 7). Throughout a duration of 150 nanoseconds, all ligand-KLK-5 complexes, with the exception of the tanshinone IIA-KLK-5 and tanshinone I-KLK-5 complexes, demonstrated a similar stability of fluctuation compared to that of the Apo structure fluctuations. The average Rg value of the Apo structure was measured at 1.2445

Å, the average Rg values for the native ligand GSK144-KLK-5, tanshinone I-KLK-5, danshensu-KLK-5, tanshinone IIA-KLK-5, azelaic acid-KLK-5, and complexes were recorded as 1.24333, 1.24747, 1.24311, 1.2498, and 1.24499 Å, respectively (Figure 7).

Ultimately, the 2D and 3D molecular interaction poses of the danshensu-KLK-5 complex, characterized by the lowest average root mean square deviation value, and the GSK144-KLK-5 complex as a reference are illustrated in Figure 8. Figure 5 and Figure 8 show that the most stable complexes, namely native ligand-KLK-5 and danshensu-KLK-5, formed
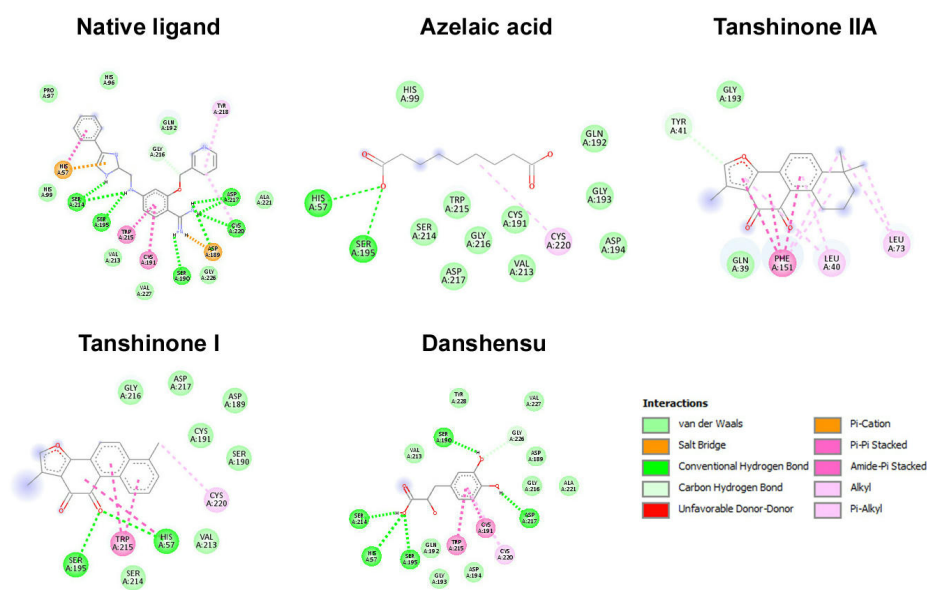
Figure 6. The 2D interaction poses of the native ligand danshensu, tanshinone IIA, tanshinone I, and azelaic acid are shown in the binding site of KLK-5.
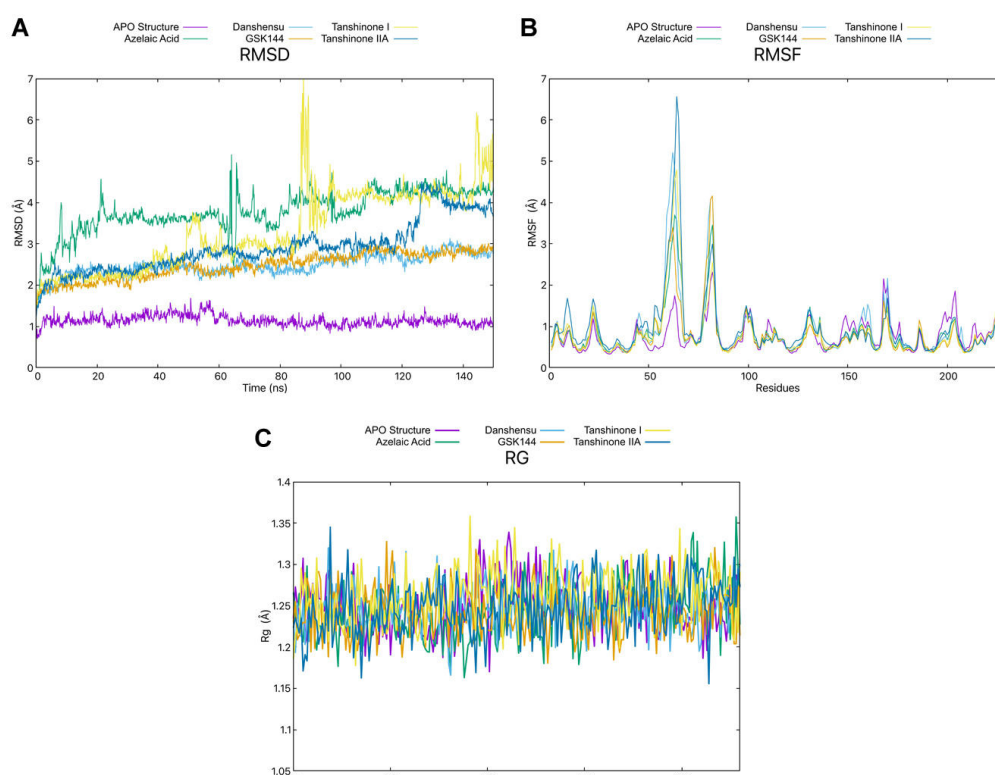

Figure 7. The RMSD (**A**), RMSF (**B**), and Rg (**C**) plots display the KLK-5 Apo structure alongside five ligand-protein complexes during the 150-ns simulation.

hydrogen bonds with similar residues observed during molecular docking. By the end of the simulation, it was noted that the native ligand formed hydrogen bonds with SER195, ASP189, VAL227, GLY193, SER214, SER190, and GLY226.

In contrast, danshensu formed hydrogen bonds with SER214, ASP189, SER195, ASP217, SER190, and GLY216.
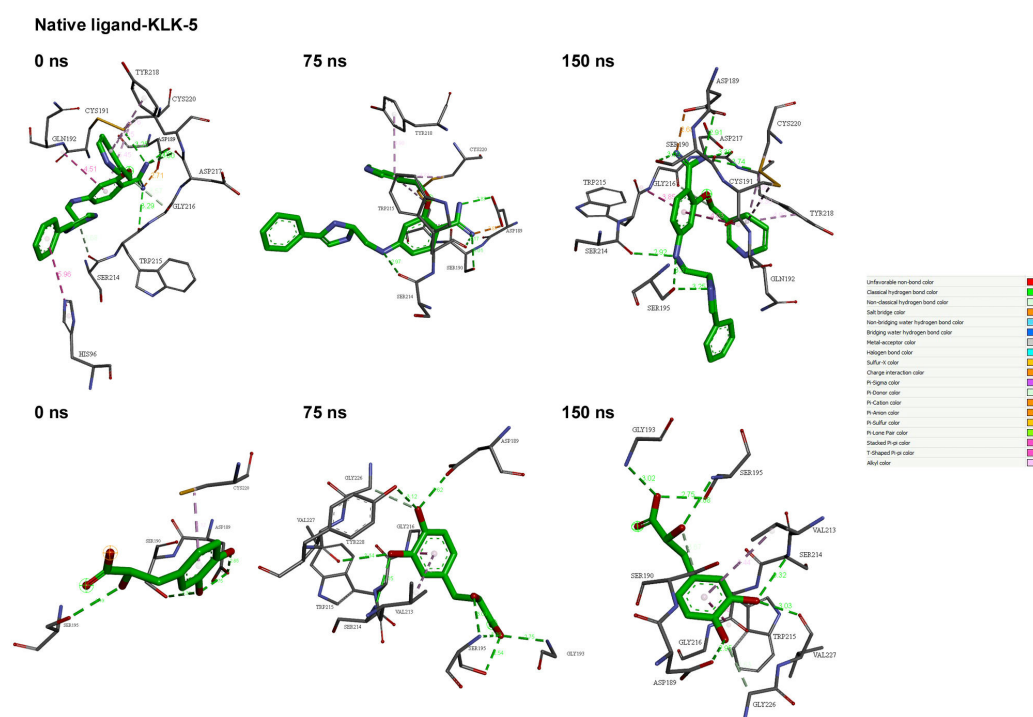
Figure 8. 3D representations of molecular interactions between the native ligand-KLK-5 and danshensu-KLK-5 complexes at 0, 75, and 150 ns.

DISCUSSION

Rosacea is a complex disease with a multifaceted pathophysiology, exhibiting clinical symptoms that reflect various morphological features across more than one subtype.[58,59] Elevated KLK-5 levels increase the antimicrobial peptide LL-37, leading to both acute and chronic inflammation in the ocular and skin areas.[6,28,29] The complicated characteristics of rosacea disease create obstacles for drug development and the effectiveness of existing therapies. Therefore, we focused on KLK-5, a stable protein that has been identified as a target in various research[7,14] involving rosacea treatments. A thorough literature review revealed that no research has been conducted on the primary phytochemical constituents of *S. miltiorrhiza* and their potential as candidates for drug development targeting KLK-5 inhibition to treat rosacea. The current study presents, for the first time, the major phytochemical components of *S. miltiorrhiza* as potential KLK-5 inhibitors, demonstrating their efficacy in treating cardiovascular, breast, oral, prostate, liver, and nervous system diseases.[60] To identify the most promising compounds for further investigation, this study utilized MD simulations, ADME-Tox analysis, and molecular docking techniques. Azelaic acid is the only FDA-approved KLK-5 inhibitor for treating rosacea[7] and served as the reference ligand in this study. Molecular docking analysis showed that phytochemical compounds from *S. miltiorrhiza* had a higher binding affinity than azelaic acid (-4.0 kcal/mol). The lower

binding energy indicates a stronger ligand affinity for the target protein. Table 1 shows that the native ligand (-9.6 kcal/mol) and key phytochemicals had higher binding affinity for KLK-5 compared to azelaic acid (-4.0 kcal/mol).

Several studies have investigated KLK-5 as a therapeutic target using different chemical strategies and validation methods. Hikmawati et al. (2022)[30] employed pharmacophore-based virtual screening and MD simulations to identify synthetic KLK-5 inhibitors from the ZINC database, reporting ZINC000022339916 as their top candidate. Similarly, Liddle et al. (2021)[61] developed a selective small-molecule KLK-5 inhibitor with demonstrated efficacy *in vitro* and *in vivo*, effectively reducing inflammation in a mouse model of Netherton syndrome through inhibition of KLK-5 activity. Walker et al. (2019)[62] synthesized tripeptidic irreversible KLK-5 inhibitors that showed substantial inhibition in enzymatic assays. White et al. (2019)[63] applied a structure-based drug design approach to develop potent KLK-5 inhibitors by combining *in silico* screening and X-ray crystallography. These studies confirmed KLK-5 as a viable therapeutic target not only in rosacea but also in other dermatological conditions, such as Netherton syndrome and atopic dermatitis. In contrast, our study is the first to explore *S. miltiorrhiza* phytochemicals as natural KLK-5 inhibitors, offering a plant-based therapeutic alternative. Among the tested compounds, danshensu stood out with a binding energy of –7.2 kcal/mol and demonstrated superior stability in MD simulations

(average RMSD: 2.48 Å, Rg: 1.24311 Å), comparable to or better than known references like the native ligand and azelaic acid. Unlike synthetic inhibitors developed in previous studies, our proposed compounds exhibit favorable ADME-Tox and pharmacokinetic profiles, with low predicted toxicity and good GI absorption, potential safety advantages. However, unlike the compounds validated experimentally in Liddle[61], Walker[62], and White's[63] work, our findings are currently limited to *in silico* predictions. Therefore, although our approach introduces a novel and potentially safer class of KLK-5 inhibitors, further *in vitro* and *in vivo* validation is essential to establish their therapeutic efficacy. In addition to favorable binding and dynamic stability, the phytochemicals identified in our study, particularly danshensu, demonstrated drug-like ADME-Tox profiles that may offer important clinical advantages over previously reported synthetic inhibitors.[64] Given the chronic nature of rosacea and the limited range of safe and effective KLK-5 inhibitors, this natural compound may represent a new generation of topical therapeutics. However, further research is needed to experimentally assess the cutaneous bioavailability and inhibitory efficacy of these agents in cellular models. Integrating formulation studies and permeability assays with *in vitro* KLK-5 activity tests would be a logical next step to confirm the therapeutic relevance of these findings.

CONCLUSION

This study examines rosacea's pathogenesis and treatment, emphasizing serine protease KLK-5's overexpression as a key management element. The complexity of rosacea complicates drug discovery and treatment efficacy. It first presents the major phytochemical components as potential KLK-5 inhibitors, showing efficacy against various diseases, including cardiovascular, breast, oral, prostate, liver, and nervous system disorders. The study utilized *in silico* methods, including molecular docking, ADME-Tox analysis, and MD simulations, to screen a library of ligands and reference compounds (such as the native ligand and azelaic acid) against KLK-5 (PDB ID: 6QFE). The binding affinities of key phytochemical compounds were assessed, excluding those with poor drug-like properties or unfavorable pharmacokinetic and physicochemical characteristics based on toxicity models predicting immunotoxicity, mutagenicity, and carcinogenicity risks. A total of 150 ns MD simulations were conducted on KLK-5 complexes with danshensu, tanshinone I, tanshinone IIA, the native ligand, and azelaic acid to confirm prior studies and assess the stability of these complexes. The analyses indicated that danshensu is the most promising compound in *S. miltiorrhiza* for inhibiting KLK-5 in treating rosacea, making it a strong candidate for further efficacy

validation. It is recommended to extend the duration of molecular dynamics simulations to stabilize the ligand-KLK-5 complexes because significant peak fluctuations were noted. Given the margin of error in in silico analyses, these findings require validation *in vitro* and *in vivo* studies. In conclusion, this study contributes to the growing body of literature on KLK-5 inhibition by introducing a novel, plant-based approach using *S. miltiorrhiza* phytochemicals. The results of this study provide a solid foundation for the future development of safe and effective KLK-5-targeted treatments for rosacea and potentially other inflammatory skin disorders.

Author Details

Sumeyye Durmaz
[1] Uskudar University, Institute of Science, Molecular Biology, Istanbul, Türkiye
🔟 0000-0002-6414-1617

Esma Ulusoy
[2] Uskudar University, Faculty of Engineering and Natural Sciences, Molecular Biology and Genetics, Uskudar, Istanbul, Türkiye
🔟 0000-0001-9925-9562   ✉ esma.ulusoy@uskudar.edu.tr

REFERENCES

1   Gether L, Overgaard LK, Egeberg A, Thyssen JP. Incidence and prevalence of rosacea: A systematic review and meta-analysis. *Br J Dermatol.* 2018;179(2):282-289.

2   Cristina Diniz Silva A, Ben Fadhel S. Ethnicity versus climate: The impacts of genetics and environment on rosacea epidemiology and pathogenesis. *Arch Clin Exp Dermatol.* 2020;2(1):109.

3   Holmes AD, Steinhoff M. Integrative concepts of rosacea pathophysiology, clinical presentation and new therapeutics. *Exp Dermatol.* 2017;26(8):659-667.

4   Rodrigues-Braz D, Zhao M, Yesilirmak N, Aractingi S, Behar-Cohen F, Bourges JL. Cutaneous and ocular rosacea: Common and specific physiopathogenic mechanisms and study models. *Mol Vis.* 2021;27:323-353.

5   Daou H, Paradiso M, Hennessy K, Seminario-Vidal L. Rosacea and the microbiome: A systematic review. *Dermatol Ther (Heidelb).* 2021;11(1). doi:10.1007/s13555-020-00460-1

6   Coda AB, Hata T, Miller J, et al. Cathelicidin, kallikrein 5, and serine protease activity is inhibited during treatment of rosacea with azelaic acid 15% gel. *J Am Acad Dermatol*. 2013;69(4):570-577.

7   Chen C, Wang P, Zhang L, et al. Exploring the pathogenesis and mechanism-targeted treatments of rosacea: Previous understanding and updates. *Biomedicines*. 2023;11(8):2153. doi:10.3390/biomedicines11082153

8   Zhang L, Wu WKK, Gallo RL, et al. Critical role of antimicrobial peptide cathelicidin for controlling *Helicobacter pylori* survival and infection. *J Immunol*. 2016;196(4):1799-1809.

9   Steinhoff M, Buddenkotte J, Aubert J, et al. Clinical, cellular, and molecular aspects in the pathophysiology of rosacea. In: *J Investig Dermatol Symp Proc*. 2011;15:2-11. doi:10.1038/jidsymp.2011.7

10 Rainer BM, Kang S, Chien AL. Rosacea: Epidemiology, pathogenesis, and treatment. *Dermatoendocrinol*. 2017;9(1):e1361574. doi:10.1080/19381980.2017.1361574

11 Gonzalez-Hinojosa D, Jaime-Villalonga A, Aguilar-Montes G, Lammoglia-Ordiales L. Demodex and rosacea: Is there a relationship? *Indian J Ophthalmol*. 2018;66(1):36-38.

12 van Zuuren EJ, Arents BWM, van der Linden MMD, Vermeulen S, Fedorowicz Z, Tan J. Rosacea: New concepts in classification and treatment. *Am J Clin Dermatol*. 2021;22(4):457-465.

13 Chang ALS, Raber I, Xu J, et al. Assessment of the genetic basis of rosacea by genome-wide association study. *J Invest Dermatol*. 2015;135(6):1548-1555.

14 Woo Y, Lim J, Cho D, Park H. Rosacea: Molecular mechanisms and management of a chronic cutaneous inflammatory condition. *Int J Mol Sci*. 2016;17(9):1562. doi:10.3390/ijms17091562

15 Cribier B. Rosacea under the microscope: Characteristic histological findings. *J Eur Acad. Dermatol Venereol*. 2013;27(11):1336-1343.

16 Rosina P, Zamperetti MR, Giovannini A, Chieregato C, Girolomoni G. Videocapillaroscopic alterations in erythematotelangiectatic rosacea. *J Am Acad Dermatol*. 2006;54(1):100-104.

17 Smith JR, Lanier VB, Braziel RM, Falkenhagen KM, White C, Rosenbaum JT. Expression of vascular endothelial growth factor and its receptors in rosacea. *Br J Ophthalmol*. 2007;91(2):226-229.

18 Kumar V. Going, Toll-like receptors in skin inflammation and inflammatory diseases. *Excli J*. 2021;20:52-79.

19 Portou MJ, Baker D, Abraham D, Tsui J. The innate immune system, toll-like receptors and dermal wound healing: A review. *Vascul Pharmacol*. 2015;71:31-36.

20 Janeway CA, Medzhitov R. Innate immune recognition. *Annu Rev Immunol*. 2002;20(1):197-216.

21 Kim JY, Kim YJ, Lim BJ, Sohn HJ, Shin D, Oh SH. Increased expression of cathelicidin by direct activation of protease-activated receptor 2: Possible implications on the pathogenesis of rosacea. *Yonsei Med J*. 2014;55(6):1648-1655.

22 Yamasaki K, Gallo RL. Rosacea as a disease of cathelicidins and skin innate immunity. *J Investig Dermatol Symp Proc*. 2011;15(1):12-15.

23 Larrick JW, Hirata M, Balint RF, Lee J, Zhong J, Wright SC. Human CAP18: A novel antimicrobial lipopolysaccharide-binding protein. *Infect Immun*. 1995;63(4):1291-1297.

24 Agerberth B, Gunne H, Odeberg J, Kogner P, Boman HG, Gudmundsson GH. FALL-39, a putative human peptide antibiotic, is cysteine-free and expressed in bone marrow and testis. *Proc Natl Acad Sci USA*. 1995;92(1):195-199.

25 Park BW, Ha JM, Cho EB, et al. A study on vitamin d and cathelicidin status in patients with rosacea: Serum level and tissue expression. *Ann Dermatol*. 2018;30(2):136-142.

26 Meyer-Hoffert U. Reddish, scaly, and itchy: How proteases and their inhibitors contribute to inflammatory skin diseases. *Arch Immunol Ther Exp (Warsz)*. 2009;57(5):345-354.

27 Fleischer AB. Inflammation in rosacea and acne: Implications for patient care. *J Drugs Dermatol*. 2011;10(6):614-620.

28 Two AM, Del Rosso JQ.. Kallikrein 5-mediated inflammation in rosacea: Clinically relevant correlations with acute and chronic manifestations in rosacea and how individual treatments may provide therapeutic benefit. *J Clin Aesthet Dermatol*. 2014;7(1):20-25.

29 Yamasaki K, Di Nardo A, Bardan A, et al. Increased serine protease activity and cathelicidin promotes skin inflammation in rosacea. *Nat Med*. 2007;13(8):975-980.

30 Hikmawati D, Fakih TM, Sutedja E, Dwiyana RF, atik N, Ramadhan DSF. Pharmacophore-guided virtual screening and dynamic simulation of Kallikrein-5 inhibitor: Discovery of potential molecules for rosacea therapy. *Inform Med Unlocked*. 2022;28. doi:10.1016/j.imu.2022.100844

31 Li J, Yuan X, Tang Y, et al. Hydroxychloroquine is a novel therapeutic approach for rosacea. *Int Immunopharmacol*. 2020;79:106178. doi:10.1016/j.intimp.2019.106178

32 Anzengruber F, Czernielewski J, Conrad C, et al. Swiss S1 guideline for the treatment of rosacea. *J Eur Acad Dermatol Venereol*. 2017;31(11):1775-1791.

33 Amir Ali A, Vender R, Vender R. The Role of IL-17 in papulopustular rosacea and future directions. *J Cutan Med Surg*. 2019;23(6):635-641.

34 Drago F, De Col E, Agnoletti AF, et al. The role of small intestinal bacterial overgrowth in rosacea: A 3-year follow-up. *J Am Acad Dermatol*. 2016;75(3):e113-e115. doi:10.1016/j.jaad.2016.01.059

35 Parodi A, Paolino S, Greco A, et al. Small intestinal bacterial overgrowth in rosacea: Clinical effectiveness of its eradication. *Clin Gastroenterol Hepatol*. 2008;6(7):759-764.

36 Rubinchik E, Dugourd D, Algara T, Pasetka C, Friedland HD. Antimicrobial and antifungal activities of a novel cationic antimicrobial peptide, omiganan, in experimental skin colonisation models. *Int J Antimicrob Agents*. 2009;34(5):457-461.

37 Salem DAB, El-shazly A, Nabih N, El-Bayoumy Y, Saleh S. Evaluation of the efficacy of oral ivermectin in comparison with ivermectin–metronidazole combined therapy in the treatment of ocular and skin lesions of *Demodex folliculorum*. *Int J Infect Dis*. 2013;17(5):e343-e347. doi:10.1016/j.ijid.2012.11.022

38 Gerber PA, Buhren BA, Steinhoff M, Homey B. Rosacea: The cytokine and chemokine network. *J Investig Dermatol Symp Proc*. 2011;15(1):40-47.

39 Asai Y, Tan J, Baibergenova A, et al. Canadian Clinical Practice Guidelines for Rosacea. *J Cutan Med Surg*. 2016;20(5):432-445.

40 Del Rosso JQ, Tanghetti E, Webster G, Stein Gold L, Thiboutot D, Gallo RL. Update on the management of rosacea from the American Acne & Rosacea Society (AARS). *J Clin Aesthet Dermatol*. 2020;13(6 Suppl):S17-S24.

41 Thiboutot D, Anderson R, Cook-Bolden F, et al. Standard management options for rosacea: The 2019 update by the National Rosacea Society Expert Committee. *J Am Acad Dermatol*. 2020;82(6):1501-1510.

42 Chen L, Tsai TF. The role of β-blockers in dermatological treatment: A review. *J Eur Acad Dermatol Venereol*. 2018;32(3):363-371.

43 Al Mokadem SM, Ibrahim ASM, El Sayed AM. Efficacy of topical timolol 0.5% in the treatment of acne and rosacea: A multicentric study. *J Clin Aesthet Dermatol*. 2020;13(3):22-27.

44 Layton AM. Pharmacologic treatments for rosacea. *Clin Dermatol*. 2017;35(2):207-212.

45 Stearns V, Slack R, Greep N, et al. Paroxetine is an effective treatment for hot flashes: Results from a prospective randomized clinical trial. *J Clin Oncol*. 2005;23(28):6919-6930.

46 Wagner KD, Berard R, Stein MB, et al. A Multicenter, randomized, double-blind, placebo-controlled trial of paroxetine in children and adolescents with social anxiety disorder. *Arch Gen Psychiatry*. 2004;61(11):1153. doi:10.1001/archpsyc.61.11.1153

47 Craige H, Cohen JB. Symptomatic treatment of idiopathic and rosacea-associated cutaneous flushing with propranolol. *J Am Acad Dermatol*. 2005;53(5):881-884.

48 Park J, Mun J, Song M, et al. Propranolol, doxycycline and combination therapy for the treatment of rosacea. *J Dermatol*. 2015;42(1):64-69.

49 Zhou L, Zuo Z, Chow MSS. Danshen: An overview of its chemistry, pharmacology, pharmacokinetics, and clinical use. *J Clin Pharmacol*. 2005;45(12):1345-1359.

50 Xu J, Wei K, Zhang G, et al. Ethnopharmacology, phytochemistry, and pharmacology of Chinese *Salvia* species: A review. *J Ethnopharmacol*. 2018;225:18-30.

51 Su CY, Ming QL, Rahman K, Han T, Qin LP. *Salvia miltiorrhiza*: Traditional medicinal uses, chemistry, and pharmacology. *Chin J Nat Med*. 2015;13(3):163-182.

52 Li X, Wang Z. Chemical composition, antimicrobial and antioxidant activities of the essential oil in leaves of *Salvia miltiorrhiza* Bunge. *J Essent Oil Res*. 2009;21(5):476-480.

53 da Silva JKR, Figueiredo PLB, Byler KG, Setzer WN. Essential oils as antiviral agents. Potential of essential oils to treat sars-cov-2 infection: An *in-silico* investigation. *Int J Mol Sci*. 2020;21(10). doi:10.3390/ijms21103426

54 Wang J, Xu J, Gong X, Yang M, Zhang C, Li M. Biosynthesis, chemistry, and pharmacology of polyphenols from Chinese *Salvia* species: A review. *Molecules*. 2019;24(1):155. doi:10.3390/molecules24010155

55 Du G, Song J, Du L, et al. Chemical and pharmacological research on the polyphenol acids isolated from Danshen: A review of salvianolic acids. *Adv Pharmacol.* 2020:1-41. doi:10.1016/bs.apha.2019.12.004

56 Shanfa L. Compendium of plant genomes. In: Shanfa L, ed. *The Salvia miltiorrhiza Genome*. Vol 1. Springer Cham; 2019:XVI-192. doi:https://doi.org/10.1007/978-3-030-24716-4

57 Wang X, Yang Y, Liu X, Gao X. Pharmacological properties of tanshinones, the natural products from *Salvia miltiorrhiza. Adv Pharmacol.* 2020;87:43-70. doi:10.1016/bs.apha.2019.10.001

58 Steinhoff M, Bergstresser PR. Pathophysiology of rosacea: Introduction. *J Investig Dermatol. Symp Proc*. 2011;15(1):1. doi:10.1038/jidsymp.2011.3

59 Wilkin JK. Rosacea. *Arch Dermatol*. 1994;130(3):359. doi:10.1001/archderm.1994.01690030091015

60 Jung I, Kim H, Moon S, Lee H, Kim B. Overview of *Salvia miltiorrhiza* as a potential therapeutic agent for various diseases: An update on efficacy and mechanisms of action. *Antioxidants*. 2020;9(9):857. doi:10.3390/antiox9090857

61 Liddle J, Beneton V, Benson M, et al. A potent and selective kallikrein-5 inhibitor delivers high pharmacological activity in skin from patients with Netherton syndrome. *J Investig Dermatol*. 2021;141(9):2272-2279.

62 Walker AL, Bingham RP, Edgar EV, et al. Structure guided drug design to develop kallikrein 5 inhibitors to treat Netherton Syndrome. *Bioorg Med Chem Lett*. 2019;29(12):1454-1458.

63 White GV, Edgar EV, Holmes DS, et al. Kallikrein 5 inhibitors identified through structure based drug design in search for a treatment for Netherton Syndrome. *Bioorg Med Chem Lett*. 2019;29(6):821-825.

64 Guan L, Yang H, Cai Y, et al. ADMET-score – A comprehensive scoring function for evaluation of chemical drug-likeness. *Medchemcomm*. 2019;10(1):148-157.